Applied Energy 106 (2013) 31–46

Contents lists available at SciVerse ScienceDirect

Applied Energy

journal homepage: www.elsevier.com/locate/apenergy

Wave power variability over the northwest European shelf seas

Simon P. Neill *, M. Reza Hashemi

School of Ocean Sciences, Bangor University, Menai Bridge, UK

HIGHLIGHTS

- We simulate the wave climate of the NW European shelf seas over a 7 year period.
- We apply a high resolution 3rd-generation wave model.
- We quantify spatial patterns of uncertainties in estimating the wave power resource.
- Uncertainty is considerably greater over winter months.
- There is a positive correlation between winter wave power and the NAO.

ARTICLE INFO

Article history:
Received 13 September 2012
Received in revised form 3 January 2013
Accepted 7 January 2013

Keywords:
Wave power
Wave climate
Wave model
Inter-annual variability
Northwest European shelf seas
North Atlantic Oscillation

ABSTRACT

Regional assessments of the wave energy resource tend to focus on averaged quantities, and so provide potential developers with no sense of temporal variability beyond seasonal means. In particular, such assessments give no indication of inter-annual variability – something that is critical for determining the potential of a region for wave energy convertor (WEC) technology. Here, we apply the third-generation wave model SWAN (Simulating Waves Nearshore) at high resolution to assess the wave resource of the northwest European shelf seas, an area where many wave energy test sites exist, and where many wave energy projects are under development. The model is applied to 7 years of wind forcing (2005–2011), a time period which witnessed considerable extremes in the variability of the wind (and hence wave) climate, as evidenced by the variability of the North Atlantic Oscillation (NAO). Our simulations demonstrate that there is much greater uncertainty in the NW European shelf wave resource during October–March, in contrast to the period April–September. In the more energetic regions of the NW European shelf seas, e.g. to the northwest of Scotland, the uncertainty was considerably greater. The winter NW European shelf wave power resource correlated well with the NAO. Therefore, provided trends in the NAO can be identified over the coming decades, it may be possible to estimate how the European wave resource will similarly vary over this time period. Finally, the magnitude of wave power estimated by this study is around 10% lower than a resource which is used extensively by the wave energy sector – the Atlas of UK Marine Renewable Energy Resources. Although this can partly be explained by different time periods analysed for each study, our application of a third-generation wave model at high spatial and spectral resolution significantly improves the representation of the physical processes, particularly the non-linear wave-wave interactions.

1. Introduction

To reduce greenhouse gas emissions and aid sustainable development, there is an urgent need to support our electricity generating capacity through the development of low carbon technologies, particularly those generated from renewable sources [1]. The ocean is a vast and largely untapped energy resource – wave energy alone has been estimated as around 2 TW globally [2]. A significant portion of this wave energy could be exploited by a range of wave energy converter (WEC) technologies [3], and so wave energy has been highlighted as a key contributor to the future global energy mix. However, progress from full-scale testing to commercialisation of wave energy projects has been relatively slow, partly due to the financial risks associated with uncertainty in quantifying the wave energy resource at a variety of timescales. This is in direct contrast to assessment of the tidal energy resource – tidal currents are largely driven by astronomical forces, and so can be accurately predicted over long time scales [4]. Beyond seasonal trends, waves are largely stochastic, and so it is difficult to quantify the long-term wave resource for a region at a variety of timescales. With likely future changes in the wave energy resource due to climate change [5–7], this uncertainty in resource assessment will increase for proposed future large-scale WEC array scenarios that have been identified in marine energy roadmaps (e.g. [8]).

* Corresponding author.
E-mail address: s.p.neill@bangor.ac.uk (S.P. Neill).

0306-2619/$ - see front matter © 2013 Elsevier Ltd. All rights reserved.
http://dx.doi.org/10.1016/j.apenergy.2013.01.026

One of the most popular data sources used by developers for quantifying the UK wave energy resource is the Atlas of UK Marine Renewable Energy Resources [9]. Similar wave resource assessments have been made for Europe [3], the Black Sea [10], the Baltic Sea [11], the Canary Islands [12], Australia [13], China [14], the United States [15], and globally [2]. Regardless of the accuracy of such studies in terms of data quality and availability, and the spatial, temporal, and spectral resolution of the underlying wave models, most assessments provide potential developers with only averaged quantities such as the annual mean significant wave height and wave power, and give no indication of temporal variability beyond seasonal means [16]. Of the few studies which do analyse how the temporal distribution of wave energy resource at seasonal and inter-annual scale affects site selection, Cornett [17] analysed variability of the global resource at a relatively coarse ($1.25^\circ \times 1^\circ$) model resolution, and Liberti et al. [18] provide a study of wave variability for the Mediterranean. Akpinar and Komurcu [10] provide a thorough resource assessment for the Black Sea, examining monthly, seasonal, and annual distributions of wave height and wave power. However, most studies give no indication of the inter-annual variability of the wave resource, something that is critical for even a superficial assessment of the wave energy potential of a region. Further, the suitability of a particular location cannot be matched to a particular WEC technology [19], since these resource assessments provide no information on the spectral properties of the waves. Rather, relatively expensive high-resolution nested model studies [20], or expensive *in situ* monitoring programmes [21], are required to make even an initial assessment of the wave energy potential of a region. The present research aims to address such issues by providing a thorough assessment of the wave energy potential of the NW European shelf seas, a region where many wave energy projects are under development. In particular, this study focusses on temporal variation of the wave resource over seasonal and inter-annual timescales, and assesses the spectral properties of the waves for a range of contrasting locations.

2. Study region

The NW European shelf sea has been selected for this study as it is one of the most energetic shelf sea regions in the world [2,22]. Due to its large wave energy resource, and the prominence of European nations (particularly the UK) in developing wave energy technologies [3], many wave energy test sites exist, and many wave energy projects are under development throughout this region, with selected sites shown on Fig. 1, and further details provided in Table 1. These eight locations form the basis of the detailed site-specific resource assessment in Section 4.2, and further details of the sites can be found in Bahaj [1], Reeve et al. [6], Mouslim et al. [23], Beels et al. [24] and Aquamarine Power [25]. These sites are located in regions of considerable variations in water depths and wave exposures, and so enable a contrast in wave properties to be made for a wide range of environments. In addition to being a suitable region for exploitation of the wave energy resource, the oceanography of the northwest European shelf seas is well documented, and extensive datasets are available, including wave buoy data, to validate models of the region. Further, since many countries have coastlines bordering the NW European shelf seas, this increases the relevance, and hence impact, of this study.

The NW European shelf seas, located on the northeastern margin of the North Atlantic, are generally shallower than 200 m (Fig. 1). The Celtic Sea, Malin Sea and northern North Sea are exposed to Atlantic waters, with water depths in the range 100–200 m, with the exception of the deeper (600 m) Norwegian Trench in the northeastern North Sea. The Celtic Sea borders the Irish Sea to the north, a semi-enclosed water body. To the east of the Celtic Sea, the English Channel connects to the southern North Sea; and to the south of the Celtic Sea lies the Bay of Biscay.

The climate of the NW European shelf is dominated by the atmospheric polar front [26]. The instability of this front causes depressions to form, tracking across the North Atlantic and following a preferred route which passes between Iceland and Scotland. There is considerable variation in the wind climate around the NW European shelf seas, but the strongest winds generally emanate from the west and south, and the mean winds from the southwest [27]. Wind speeds tend to be highest to the northwest of the British Isles (closest to the depression tracks), decreasing towards the south and east. An annual cycle of higher wind speeds in winter and lower speeds in summer reflects the seasonally varying strength of the large-scale atmospheric circulation [26]. The strong background flow leads to high mean wave energy over the shelf seas and the variability results in a wave climate with considerable extremes [28]. Considerable interannual variability in the synoptic-scale circulation over the Atlantic is described by the North Atlantic Oscillation (NAO) index [29], and a previous study has demonstrated that there is a positive correlation between the NAO and the mean wave power for an area off the north coast of Scotland [30]. In regions of the shelf seas exposed to the Atlantic, the orbital velocity of the longer-period (swell) waves penetrates to the sea bed [31]. Where fetch length is sufficient, the wave distribution over the shelf seas broadly maps to the wind distribution [28]. Due to the dominant southwesterly wind direction, many regions of the NW European shelf seas are relatively sheltered from wind effects and hence experience relatively low wave energy, particularly the western seaboard of the North Sea (sheltered by the UK land mass) and the northern half of the Irish Sea (sheltered by Ireland).

3. Methods

3.1. Wave model

The third-generation spectral wave model SWAN (Simulating Waves Nearshore) was used to simulate wave climates over the North Atlantic, including the NW European shelf seas. SWAN is an Eulerian formulation of the discrete wave action balance equation [32]. The model is spectrally discrete in frequencies and directions, and the kinematic behaviour of the waves is described by the linear theory of gravity waves. SWAN accounts for wave generation by wind, non-linear wave-wave interactions, white-capping, and the shallow water effects of bottom friction, refraction, shoaling, and depth-induced wave breaking.

The evolution of the action density N is governed by the wave action balance equation which, in spherical coordinates, is [32]

$$\frac{\partial N}{\partial t} + \frac{\partial c_\lambda N}{\partial \lambda} + \frac{\partial c_\phi N}{\partial \phi} + \frac{\partial c_\sigma N}{\partial \sigma} + \frac{\partial c_\theta N}{\partial \theta} = \frac{S_{tot}}{\sigma} \quad (1)$$

where c_λ and c_ϕ are the propagation velocities in the longitude (λ) and latitude (ϕ) directions, σ is frequency, θ is wave direction, and S_{tot} represents the source terms, i.e. generation, dissipation, and non-linear wave-wave interactions. For this application, the wave energy spectrum at each grid point was divided into 40 discrete frequency bins and 45 discrete direction bins for both scales of model simulation (North Atlantic and NW European shelf seas – see Section 3.3). The lowest modelled frequency was 0.05 s^{-1} (period T = 20 s), and the highest frequency resolved by the model was 2 s^{-1} (T = 0.5 s). Outside of this range, the wave spectrum was imposed, hence the effects of lower and higher frequencies are included in the simulations [33].

Version 40.85 of SWAN was run in third-generation mode, with Komen linear wave growth and whitecapping, and quadruplet

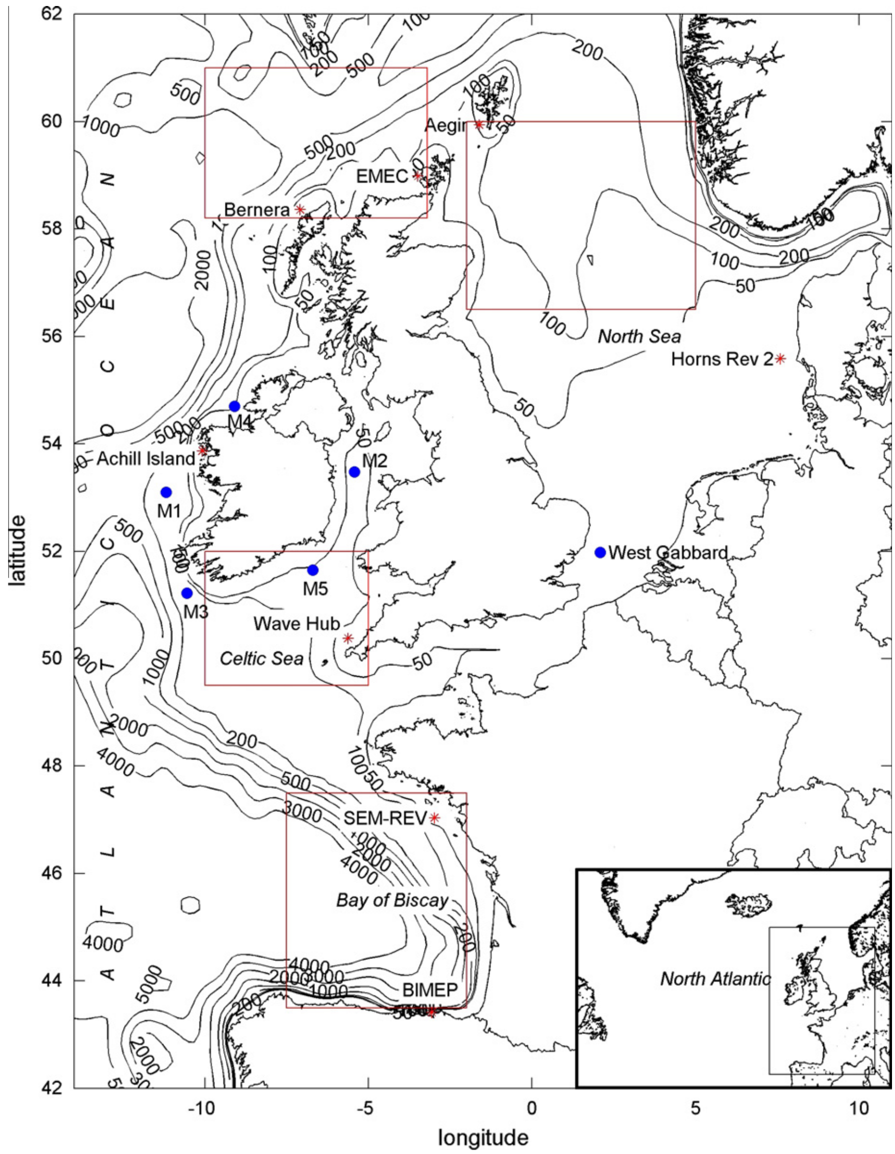

Fig. 1. Locations of selected wave energy projects and test sites distributed around the NW European shelf seas in regions of contrasting exposure, water depths, and wave climates. Blue circles (labelled) are the wave buoys used for model validation (further details are provided in Table 2), and the boxed regions are the areas used for regional comparisons (Biscay, Celtic, North Scotland and North Sea). Contours show water depth in metres relative to mean sea level. The inset which covers the entire North Atlantic shows the limits of the $1/6^\circ \times 1/6^\circ$ (outer) wave model which was run initially to generate boundary conditions for the $1/24^\circ \times 1/24^\circ$ (inner) nested wave model. (For interpretation of the references to colour in this figure legend, the reader is referred to the web version of this article.)

wave-wave interactions. Due to the scale of the simulations, bottom friction, depth-induced wave breaking, and triads were turned off. SWAN default formulations and coefficients were used for all of the physical processes.

3.2. Data sources

3.2.1. Bathymetry

GEBCO (General Bathymetric Chart of the Oceans) gridded bathymetry data was obtained from the British Oceanographic Data Centre (BODC) at a resolution of 30 arc-seconds in both latitude and longitude. This data was bi-linearly interpolated to the desired resolution of the computational domain (Section 3.3).

3.2.2. Wind data

Gridded wind data was provided by Met Éireann (the Irish Meteorological Service) using their operational HIRLAM (High Resolution Limited Area Model) version 7.2 forecast model (www.hirlam.org). The grid resolution of the model is $0.1^\circ \times 0.1^\circ$, with 60 vertical levels, and the resolution of the interpolated output wind data is $0.5^\circ \times 0.5^\circ$, extending from 60°W to 15°E, and from 40°N to 70°N. Data was available 3-hourly from January 2005 to December 2011.

Table 1
Locations of wave energy projects and test sites used for detailed analysis.

Project	Lat	Long
BIMEP (Spain) – Biscay Marine Energy Platform	43.42	−3.07
SEM-REV (France) – wave energy test site	47.04	−2.98
Wave Hub (England)	50.38	−5.63
Horns Rev 2 (Denmark) – wind farm	55.58	7.59
Aegir (Shetland) – Pelamis	59.94	−1.62
EMEC (Orkney)	58.98	−3.49
Bernera (Scotland) – Pelamis	58.36	−7.09
Achill Island (Ireland) – Aquamarine Power	53.87	−10.08

Table 2
Model performance for *Hs* and *Tp* at various locations around the NW European shelf seas. Results are generally reported for an entire year of data and, in addition, results are reported seasonally for the M1 wave buoy to demonstrate temporal differences in model/data comparison.

Reference	Water depth (m)	Lat	Long	*Hs*			*Tp*		
				RMSE (m)	SI	Bias (m)	RMSE (s)	SI	Bias (s)
M1-2005	124	53.10	−11.19	0.50	0.17	−0.22	1.10	0.15	−0.42
M1 – D-J-F 2005				0.65	0.22	−0.36	1.25	0.18	−0.79
M1 – M-A-M 2005				0.47	0.16	−0.19	1.06	0.15	−0.28
M1 – J-J-A 2005				0.33	0.11	−0.15	0.95	0.14	−0.23
M1 – S-O-N 2005				0.53	0.18	−0.19	0.97	0.14	−0.40
M2-2005	73	53.48	−5.43	0.31	0.26	−0.16	0.82	0.19	0.53
M3-2005	126	51.22	−10.55	0.51	0.18	−0.24	1.17	0.17	−0.40
M4-2005	50	54.70	−9.09	0.62	0.26	0.17	1.06	0.16	−0.18
M5-2005	65	51.65	−6.70	0.59	0.36	0.39	0.94	0.18	0.21
W Gabbard – 2007	34	51.98	2.08	0.28	0.25	−0.09	1.14	0.21	−0.64

3.2.3. Wave data

Data from five wave buoys was obtained from the Irish Marine Institute, and data from an additional wave buoy operated by Cefas (Centre for Environment, Fisheries and Aquaculture Science) was obtained from BODC to provide validation for the North Sea. These wave buoys are located in a range of water depths and wave exposures (Table 2), and so provide a rigorous validation test over a range of environments. Data of significant wave height (*Hs*) and peak wave period (*Tp*) was available hourly throughout 2005 for the Irish Marine Institute wave buoys, and half-hourly throughout 2007 for the Cefas wave buoy.

3.3. Implementation of the wave model

The wave model was applied initially to a region which included the entire North Atlantic at a grid resolution of $1/6° \times 1/6°$, extending from 60°W to 15°E, and from 40°N to 70°N (i.e. the same domain covered by the gridded wind data) (see the inset on Fig. 1). Two-dimensional (2D) wave spectra were output hourly from this coarse outer grid simulation and interpolated to the boundary of an inner nested high resolution model of the NW European shelf seas. This inner nested region had a grid resolution of $1/24° \times 1/24°$, extending from 14°W to 11°E, and from 42°N to 62°N. After running the coarser outer model of the North Atlantic, this inner nested simulation was run without feedback to the outer nest, i.e. the nesting process was one-way. Variables were output every 3 h from this nested simulation at every grid point. One-dimensional (1D) and 2D wave spectra were also output at various locations where the spectral properties of waves were to be examined (Table 1). The period 2005–2011 was simulated, corresponding to the period of the available wind data. It took approximately 35,000 CPU hours to perform all of the model simulations, using 96 cores of a 2072 core system, based on Intel Xeon processors.

To demonstrate that the selected years of simulation (2005–2011) were representative of temporal variability over the study region, we made use of the ERA-Interim dataset (available 6-hourly at a grid resolution of $1.5° \times 1.5°$) over the North Atlantic, a dataset that has been successfully applied in previous studies of wave energy flux [34]. The ERA-Interim data were used to calculate the mean value of Hs^2 (a proxy for wave energy) over the North Atlantic (from 60°W to 15°E, and from 40°N to 70°N) every 6 h from 1979 to 2011. The statistical properties of Hs^2 were then calculated for different time periods to check for stationarity in the data. The mean $\bar{x} = 9.93\ \mathrm{m}^2$ and standard deviation $s = 7.02\ \mathrm{m}^2$ were calculated for the time period 1979–2004. The corresponding values for the time period 1979–2011 (i.e. extending the analysis to incorporate our modelled time period) were $\bar{x} = 9.99\ \mathrm{m}^2$ and $s = 6.98\ \mathrm{m}^2$, i.e. differences of around 0.6% from the time period 1979 to 2004. Finally, $\bar{x} = 10.21\ \mathrm{m}^2$ and $s = 6.82\ \mathrm{m}^2$ were calculated for the time period 2005–2011, differences of around 2% from calculations for the 1979 to 2011 time period. Since these differences in statistical properties between each of the time periods was very small, our modelled time period (2005–2011) can be regarded as a representative sample of the wave power.

3.4. Model validation

The model was validated throughout 2005 using hourly time series of *Hs* and *Tp* from five wave buoys, and throughout 2007 for an additional (half-hourly) wave buoy located in the North Sea (Table 2). Good agreement was obtained for *Hs* (Fig. 2), with an average root mean square error (RMSE) of 0.47 m across all wave buoys (Table 2). Also reported on the table are the scatter index SI (RMSE normalised by the mean of the observations), and bias (mean error, calculated as model results minus observations). The SI for *Hs* was generally less than 0.25, with a peak value of 0.36 at the M5 buoy in the southern Irish Sea. The calculations of bias indicate that there was no systematic error in modelled *Hs*, with a mean value across all six wave buoys of −0.03 m. To assess the temporal variability in model performance, we also report seasonal values of RMSE, SI and bias for the M1 buoy (Table 2). Although we do find slightly larger RMSE (and SI) during autumn and winter months, these increased values are consistent with the increased uncertainty in wave power which occurs over these months (Section 4.1). There was considerably more variability in *Tp* at all of the validation locations (Fig. 3), but the model was generally in good agreement with the data, successfully reproducing variability at seasonal and sub-seasonal timescales. The average RMSE for *Tp* was 1.04 s across all sites (Table 2), but the values of SI were generally lower than the corresponding SI for *Hs*. Again, there was no particular bias in the modelled *Tp*, and there were increased errors during winter months, consistent with increased uncertainty in wave power during these more energetic periods.

4. Results

4.1. Wave power

Much of the subsequent analysis is based on wave power, which was calculated using linear wave theory. For a sinusoidal wave, the total (potential plus kinetic) time-averaged energy per unit horizontal area is

$$E = \frac{1}{8}\rho g H^2 \tag{2}$$

Since $H = \sqrt{2}Hs/2$, then wave energy

$$E = \frac{1}{16}\rho g Hs^2 \tag{3}$$

Wave energy is transported at the group velocity, c_g, and so the wave energy flux, or wave power P, can be calculated using

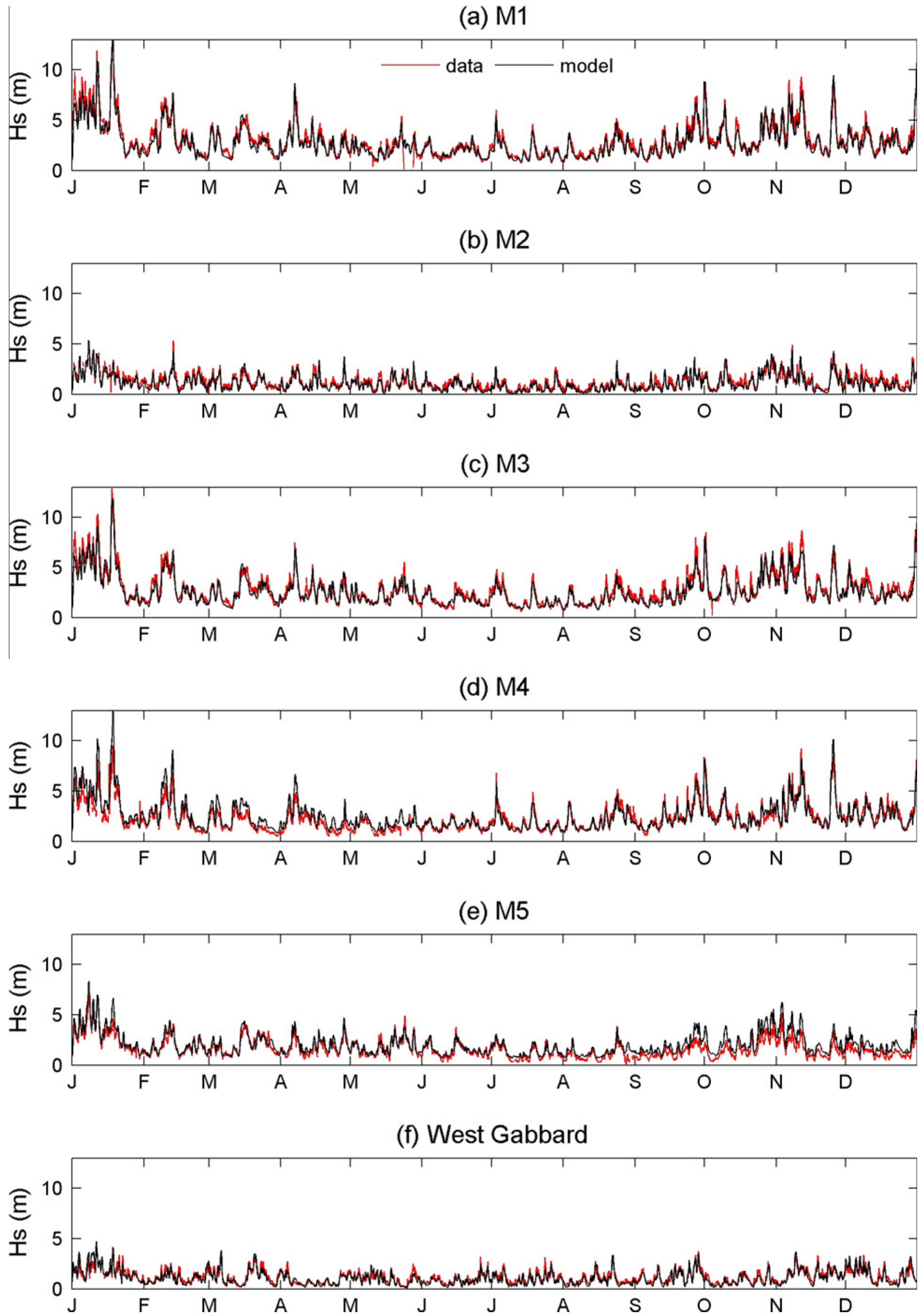

Fig. 2. Comparison of observed and modelled significant wave height for six locations distributed around the NW European shelf seas.

$$P = \frac{1}{16}\rho g H s^2 c_g \quad (4)$$

Results of the monthly mean wave power for a typical year (2007) are given in Fig. 4. It is difficult to define what a typical year actually is, but 2007 was typical in that wave power was greatest during the winter months (December–January–February), and at a minimum during the summer months (June–July–August). However, several anomalies exist, typical of multi-year/multi-seasonal datasets. For example, wave power during March (a spring month) was greater than February (a winter month). It is also interesting to note the differences in the geographic distribution of wave power between the peak months of January, February, March and December. In January and March, peak wave power was located to the northwest of Scotland and Ireland. In contrast, the wave power in February was more focussed on the Celtic Sea and Bay of Biscay, while during December this distribution extended further north than the February distribution to encompass the west coast of Ireland. However, the objective of this paper is not to discuss any particular year in detail, but to examine inter-seasonal and inter-annual variability. It is therefore more useful to consider seasonally- and annually-averaged quantities.

The seasonal and annual distribution of wave power is summarised qualitatively in Fig. 5. With the exception of 2010, the wave resource was greatest in the winter months (December–January–February), and tended to be concentrated in waters exposed to the North Atlantic, particularly the northwest of Scotland and Ireland, and the west coast of Ireland, occasionally extending into the Celtic Sea and Bay of Biscay. With very few exceptions, the

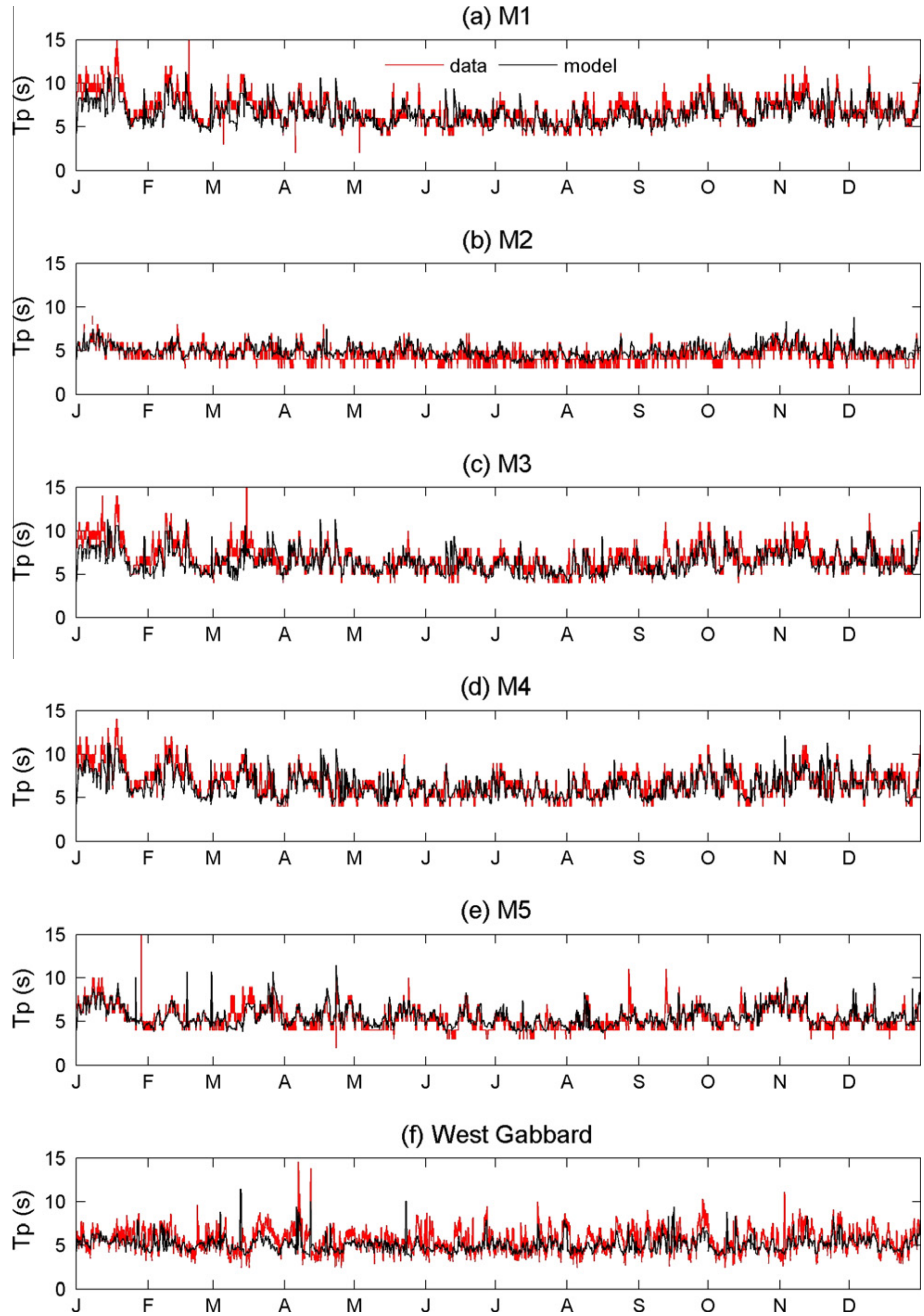

Fig. 3. Comparison of observed and modelled peak wave period for six locations distributed around the NW European shelf seas.

Autumn (September–October–November) resource was greater than the Spring (March–April–May) resource, and wave power was always at a minimum during the summer months (June–July–August). There was considerable variation between years, with 2010 being the least energetic year, and 2011 being the most energetic year.

To quantify the above results, the mean wave power was calculated over the NW European shelf seas for each season (Fig. 6). Averages, based on all of the data, provide a context (Table 3). Generally, wave power over the NW European shelf seas was around 48 kW/m in the winter, reducing to 11 kW/m in the summer. There were considerable extremes in the winter wave power, ranging from 29 kW/m in 2010 to 59 kW/m in 2007. Indeed, in 2010 the autumn wave power (34 kW/m) actually exceeded the winter wave power. However, when averaged over the whole year, there is significantly less variability of the wave resource – the annual mean wave power ranged from 23 to 33 kW/m over the NW European shelf seas, compared to a mean for all simulated years of 29 kW/m. The annual fluctuation of wave power over the NW European shelf seas is shown on Fig. 7, including 90% confidence intervals calculated using all 7 years of model output. There is clearly much greater uncertainty over the winter months, plus early spring (March) and mid to late autumn (October and November), compared to the less variable April–September period. The uncertainty from October–March is ±3.9 kW/m (compared to an October–March mean wave power of 43 kW/m), in contrast to an

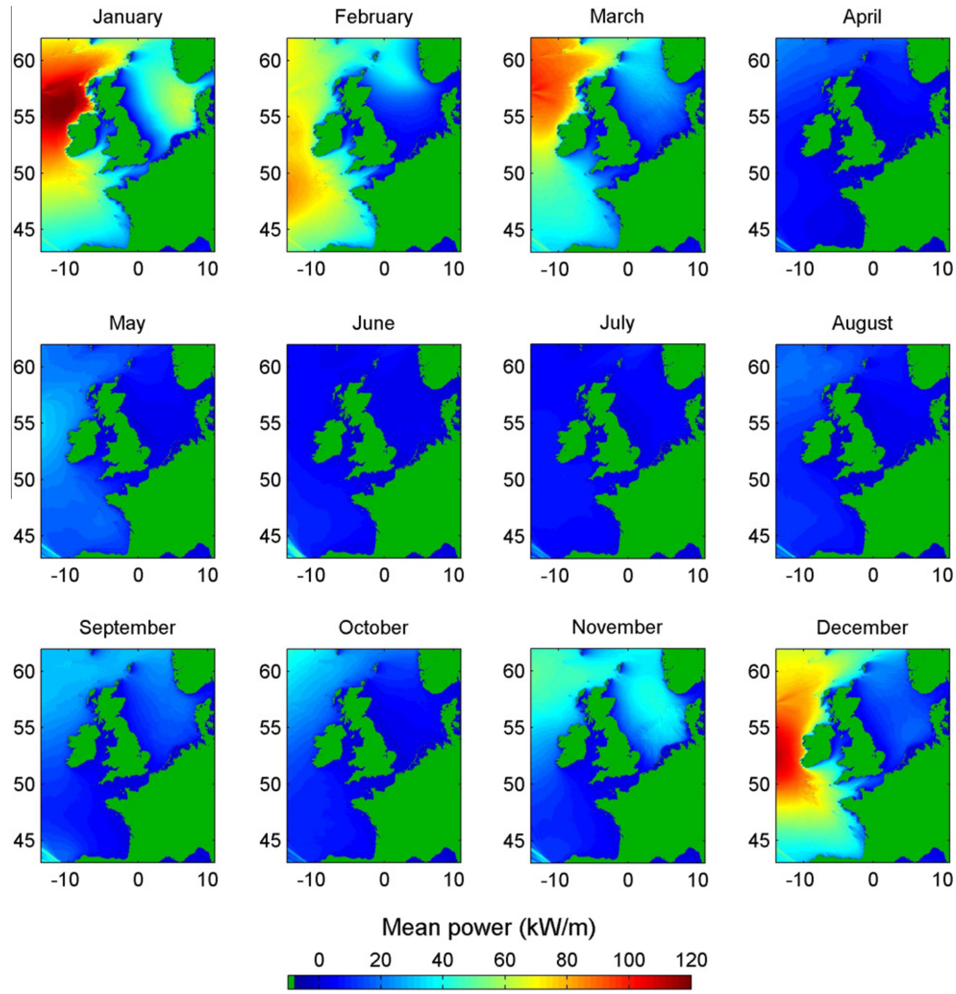

Fig. 4. Spatial distribution of mean monthly wave power throughout 2007.

April–September uncertainty of ±1.4 kW/m (compared to an April–September mean of 15 kW/m). It is therefore important to consider whether electricity supply for a region needs to be matched to demand in either winter (e.g. for heating) or summer (e.g. for cooling). If wave power is to be relied on as a key contributor to the future energy mix for Europe from October–March, there is considerable risk in the reliability (i.e. predictability) of the resource during this period, particularly on a month-by-month basis.

From Fig. 5, it is clear that there are significant regional variations in the European wave power resource, and these have not been accounted for in the shelf-scale analysis presented above. Four contrasting shelf sea regions were therefore selected, representing a spatial contrast in the wave resource. These four regions (Biscay, Celtic, North Scotland and North Sea) are shown on Fig. 1. The mean wave power was calculated over each of these shelf sea regions for each year and for each season (Fig. 8). Again, seasonal/annual averages calculated for all years for each of these regions (Table 3) provide a context. As expected from the previous analysis, the north of Scotland contains the greatest wave resource with a typical annual mean of 44 kW/m, almost double the next highest region (Celtic at 26 kW/m). In terms of seasonal variability between these regions, it is useful to examine uncertainty over the time period October–March (Fig. 9), when the shelf-scale variability was greatest, and corresponding to the time when wave power is at its peak. To the north of Scotland, the October–March uncertainty in wave power was ±10.7 kW/m (compared to an October–March mean wave power of 68 kW/m), in contrast to an April–September uncertainty of ± 2.7 kW/m (compared to an April–September mean wave power of 21 kW/m). It is also interesting to note the high uncertainty in October to the north of Scotland (±15.8 kW/m, compared to a mean October wave power resource of 51 kW/m), since this high October uncertainty is unique over the four regions examined in detail. To examine the spatial distribution of wave power variability in more detail, seasonal and annual means, uncertainty, and uncertainty expressed as a percentage of the mean wave power, were calculated for the entire model domain (Fig. 10). Although the regions to the northwest of Scotland and west of Ireland are associated with the highest uncertainty, particularly during winter months, various other regions have a high uncertainty when expressed as a percentage of the mean wave power. The spatial distribution of this quantity tends to change seasonally, and so is not fully reflected in the annual percentage uncertainty. For example, during March–April–May, there is a high percentage uncertainty in the western part of the North Sea, with low percentage uncertainty in the Irish Sea. In June–July–August, this pattern is reversed with low percentage uncertainty in the western North Sea, and high percentage uncertainty in the Irish Sea. Although these regions are associated with some of the most reliable wave resources throughout the year, the wave power in these regions is relatively low.

4.2. Wave spectra

Knowledge of the spectral properties of waves is important when attempting to match a WEC technology with the wave

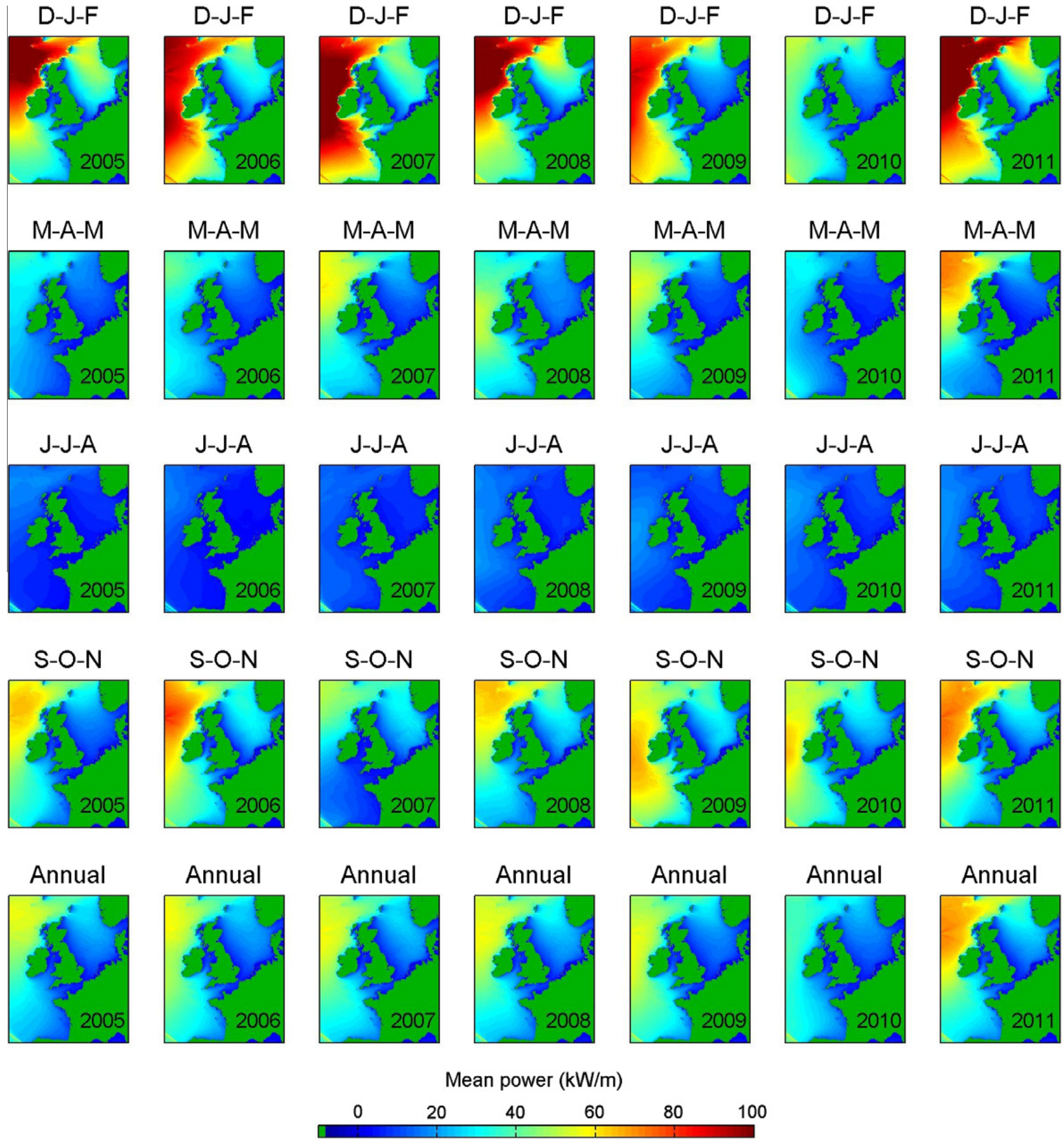

Fig. 5. Spatial distribution of seasonal and annual mean wave power for all simulated years.

climate at a particular location. Therefore, wave spectra were output from the model every 3 h for the eight locations listed in Table 1, and used to calculate annual and seasonal means for each year of simulation. To give us confidence in the simulated wave spectra, we qualitatively compared outputs of the one-dimensional (1D) and 2D wave spectra with data available for the Wave Hub site [35]. Comparing over a range of conditions with varying complexity (e.g. swell-dominated and bi-modal spectra), the 1D and 2D spectra produced by the model compared well with the observations, in terms of frequency, direction, and the magnitude of spectral density. The annual mean (1D) wave spectra for the eight locations are shown in Fig. 11. Clearly, Aegir, Bernera and Achill Island are the most energetic sites, located to the west of Ireland and northwest of Scotland, where peak wave power tends to occur over the NW European shelf seas (Fig. 5). Fig. 11 reflects the low wave energy which occurred in 2010 (largely due to a quiescent winter), and demonstrates the range of inter-annual variability. In Bernera, for example, a peak spectral density of 5.4 m^2 s (averaged over a year) occurred in 2011, yet in the previous year (2010) the peak was only 2.2 m^2 s. The winter (December–January–February) mean 1D wave spectra (Fig. 12) follow a similar trend. It is interesting to note that the peak wave frequency does not vary considerably from year-to-year, regardless of whether the mean is calculated over the entire year, or only over winter months. Table 4 shows the peak wave period at each location for each year of simulation, listed as both the annual and winter mean. In some years, and for some locations, e.g. Wave Hub in 2010, the annual mean of the peak wave period (Tp = 9.6 s) actually exceeded the winter mean (Tp = 6.6 s), indicating the importance of swell waves throughout the year. However, 2010 was an exceptionally quiescent winter in terms of the wave power resource (Fig. 5).

Typical annual mean 2D wave spectra are shown in Fig. 13, demonstrating variability in the directionality of wave energy between locations. Generally, the peak direction is aligned with the predominant wind (and hence wave) direction, reflecting both the geographic location with respect to the larger-scale North Atlantic climate system, and wave refraction in intermediate water depths. For example, there are very clear refraction effects over the

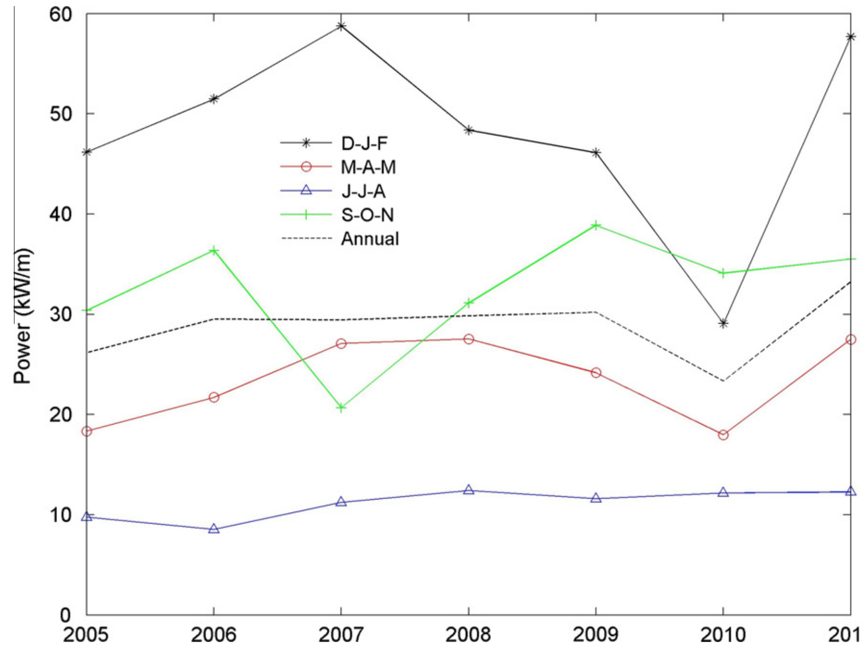

Fig. 6. Seasonal and annual mean wave power over the NW European shelf seas calculated for each simulated year.

Table 3
Calculated wave power (in kW/m) from 2005 to 2011 for regions of the NW European shelf seas: seasonal and annual means, plus 90% confidence intervals.

Region	Mean wave power				
	Winter	Spring	Summer	Autumn	Annual
Entire shelf seas	48.2 ± 7.3	23.5 ± 3.1	11.1 ± 1.1	32.4 ± 4.4	28.8 ± 2.3
Biscay	39.8 ± 7.1	18.2 ± 3.3	7.5 ± 1.5	23.9 ± 6.3	22.3 ± 2.3
Celtic	46.0 ± 11.4	20.1 ± 3.8	9.3 ± 2.1	28.4 ± 8.1	25.9 ± 3.4
N Scotland	76.6 ± 15.2	37.3 ± 7.8	13.4 ± 1.1	50.5 ± 5.6	44.4 ± 5.8
N Sea	36.9 ± 6.2	16.2 ± 2.0	8.4 ± 1.4	27.9 ± 2.2	22.4 ± 2.1

relatively shallow shelf at BIMEP and Wave Hub, but the sites to the west of Ireland and northwest Scotland (e.g. Bernera and Achill Island) are relatively unaffected by refraction, since there is a very narrow shelf between these sites and the long period waves propagating from the North Atlantic. It is also interesting to note from Fig. 13 that at Horns Rev 2, although the wave resource is relatively low, the spectral peak is strongly bi-modal, reflecting the different modes of wave climate that are responsible for generating most of the wave energy at this site. Also reported on Fig. 13 is mean directional spread. Directional spread provides a measure of dispersion around the mean wave direction, and is defined as the standard deviation of the wave direction distribution, or directional standard deviation. The directional spread across the sties ranges from 21.3° (BIMEP) to 29.7° (Aegir). These values demonstrate that whereas the peak wave direction is generally narrowly defined at each of the locations, there is a significant quantity of wave energy distributed over a much larger range of directions, particularly at

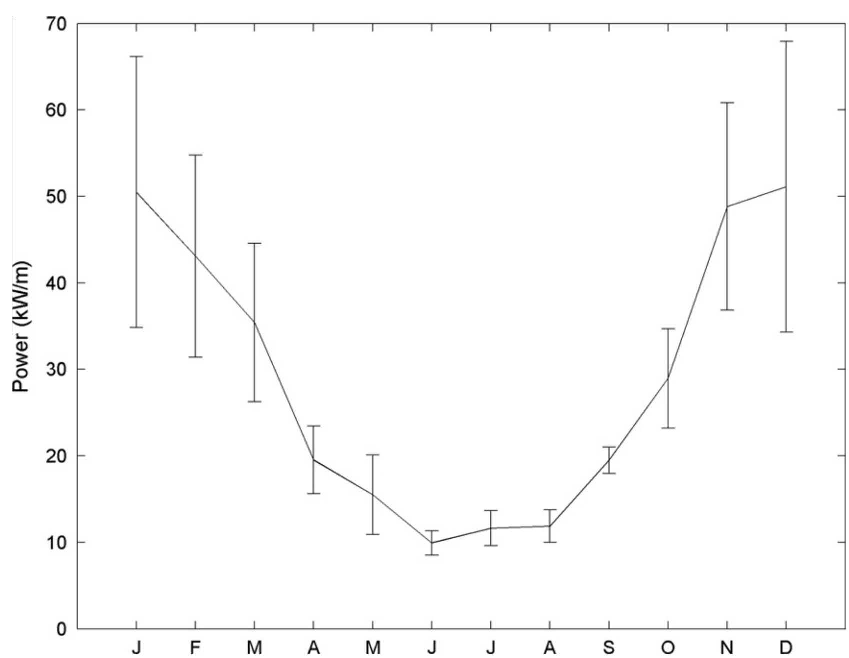

Fig. 7. Annual cycle of monthly mean wave power over the NW European shelf seas. Error bars show the 90% confidence intervals.

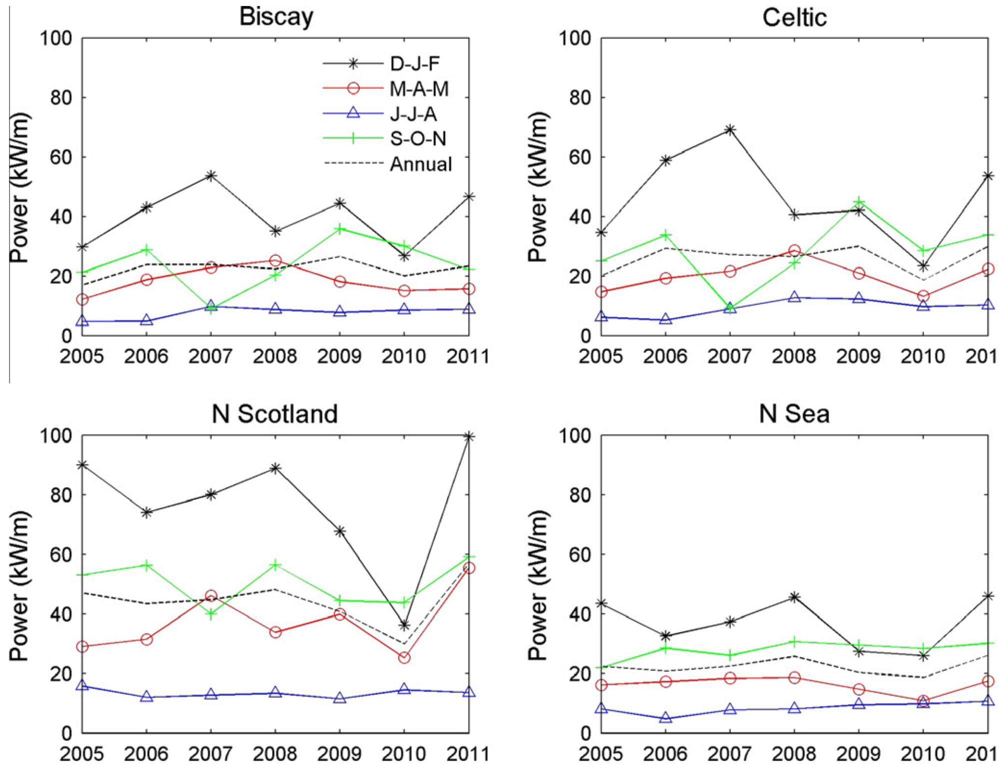

Fig. 8. Seasonal and annual mean wave power over regions of the NW European shelf seas calculated for each simulated year.

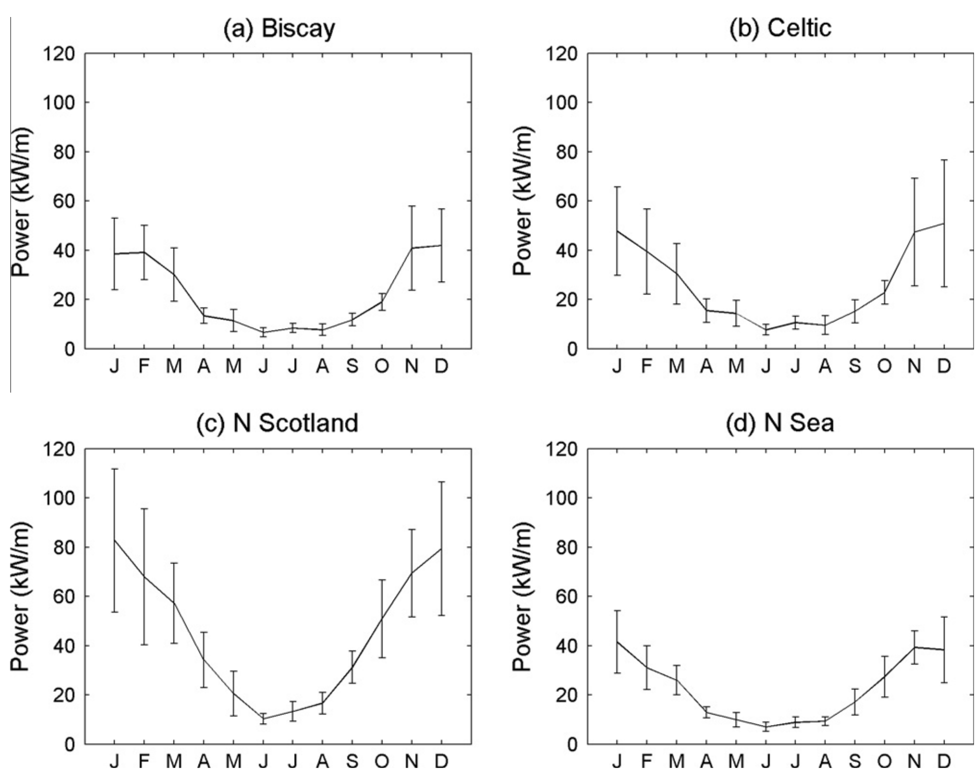

Fig. 9. Annual cycle of monthly mean wave power over regions of the NW European shelf seas. Error bars show the 90% confidence intervals.

the more exposed sites. Knowledge of this statistic enables developers to select devices appropriate to the expected spread of wave energy, and provides a more realistic assessment of how wave power propagates in relation to the mean wave direction [2].

5. Discussion

As expected, the largest wave power resource occurred during winter months December–January–February (48 kW/m averaged

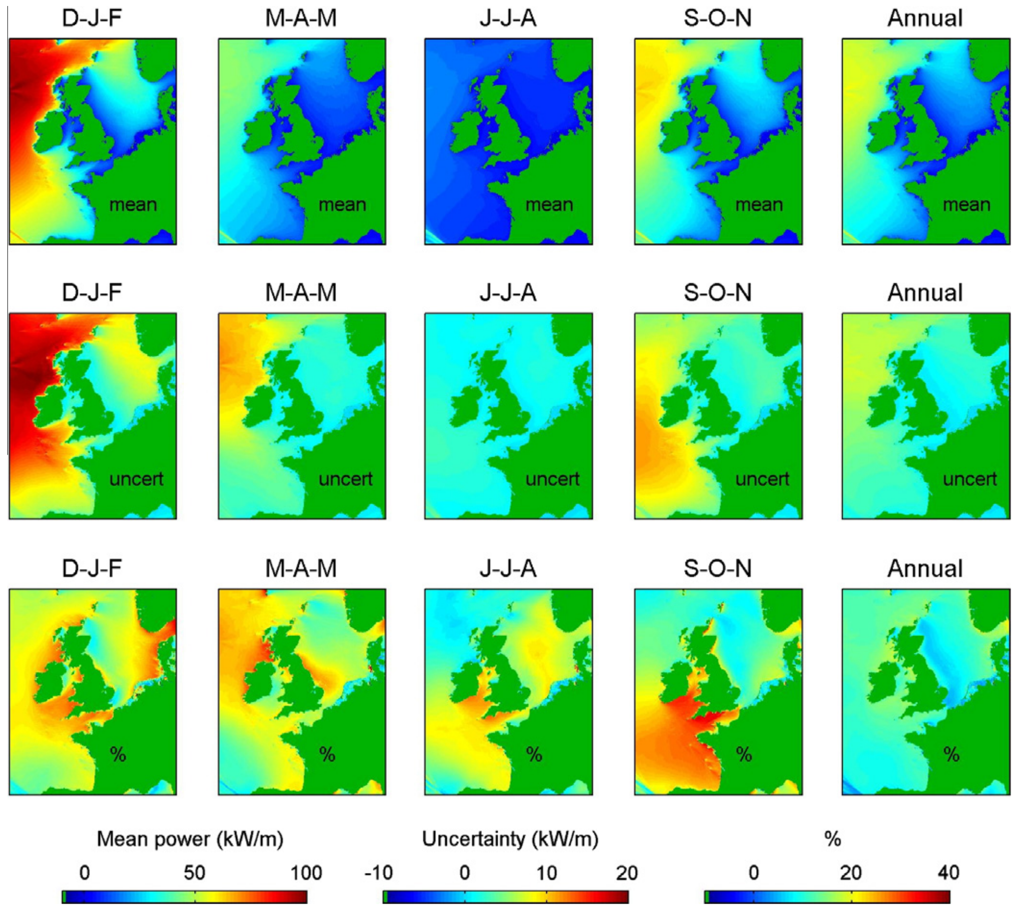

Fig. 10. Seasonal and annual distribution of mean wave power, wave power uncertainty (90% confidence), and uncertainty expressed as a percentage of mean wave power.

over the NW European shelf seas for all years), with a minimum during the summer months June–July–August (11 kW/m). Further, the wave resource during the autumn months September–October–November (32 kW/m) was considerably greater than the spring (March–April–May) resource (24 kW/m). Although the uncertainty in annual wave power over the shelf seas was relatively small (±2.3 kW/m, relative to an annual mean of 29 kW/m), the uncertainty was much greater during winter months (±7.3 kW/m, relative to a winter mean of 48 kW/m). There was considerably less uncertainty in wave power over the summer months (±1.1 kW/m, relative to a summer mean of 11 kW/m). Since swell waves are still present during summer months, and wave power is still appreciable in some regions of the NW European shelf seas during summer, this has relevance to the reliability of the wave resource in providing electricity for cooling during the summer, an issue which is likely to be exacerbated in the future under a changing climate [36]. In general, the results of this study show that uncertainty in the wave resource is relatively high during October–March, and relatively low during April–September. Further, in more energetic regions of the NW European shelf seas (e.g. to the northwest of Scotland), the uncertainty is much greater (±15.2 kW/m over the winter months, compared to a winter mean of 77 kW/m). A previous study of this region to the north of Scotland, based on analysis of a single point of a relatively coarse wave model, indicated that inter-annual variability of wave energy yield (for a Pelamis device) was around 360–720 kW in the winter, reducing to around 90–330 kW in summer [30]. The Bay of Biscay and the northern part of the North Sea, although not particularly energetic regions with typical annual mean wave powers of around 22 kW/m, have relatively low uncertainties (around ±2 kW/m), and so could provide a reliable source of wave energy for a device/array which is tuned to the appropriate wave frequencies.

5.1. The North Atlantic Oscillation

The North Atlantic Oscillation (NAO) is a large-scale mode of natural climate variability that has important impacts on the climate of northern Europe [37]. Although the NAO can be calculated throughout the year, it is during the winter months that it is particularly dominant, corresponding to the months when wave power generally peaks over the NW European shelf seas (Fig. 7). To help explain the inter-annual variability of the NW European shelf sea wave resource, the December–January–February (DJF) mean wave power over the shelf seas was plotted against the DJF NAO, using data available from the Climatic Research Unit at the University of East Anglia. There is a large range of the NAO over our modelled time period, ranging from −3.1 (generally anticyclonic) to +1.8 (mostly strong westerlies), representing a considerable range of climatic conditions with which to test the relationship between wave power and the NAO. There is good agreement (coefficient of determination $r^2 = 0.69$) between wave power and the NAO (Fig. 14), and the positive gradient indicates that winter wave power will be relatively high (e.g. >60 kW/m) over the NW European shelf seas for strongly positive DJF NAO years, and the winter wave power will be relatively low (e.g. <30 kW/m) for strongly negative DJF NAO years. Therefore, in support of other research which has correlated wave power with the NAO [30], this study demonstrates that the NAO is a useful tool

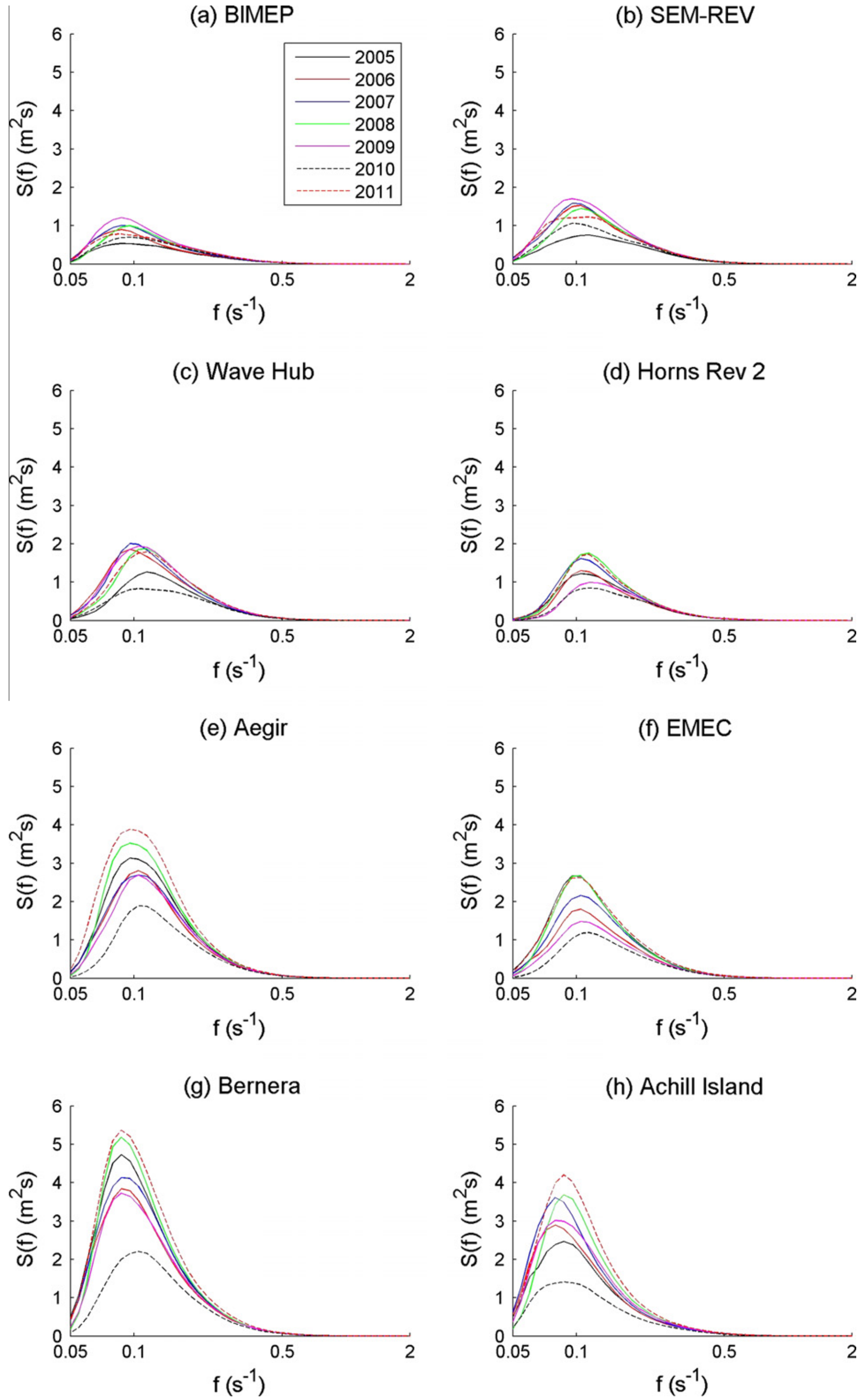

Fig. 11. One-dimensional annual mean wave spectra for eight locations distributed around the NW European shelf seas.

to determine how the winter NW European shelf wave energy resource will vary over the coming decades, provided trends in the NAO can be identified with any certainty. Although annual forecasts of the NAO are not reliable due to the high uncertainty associated with global circulation model predictions, it is a useful indice for predicting variability over longer time periods (e.g. multi-annual to multi-decadal) [38].

5.2. Comparison with the Atlas of UK Marine Renewable Energy Resources

How do our results compare with those presented in the Atlas of UK Marine Renewable Energy Resources [9] – a resource which is used extensively by the wave energy sector? The Atlas is restricted to the UK continental shelf and channel islands territorial

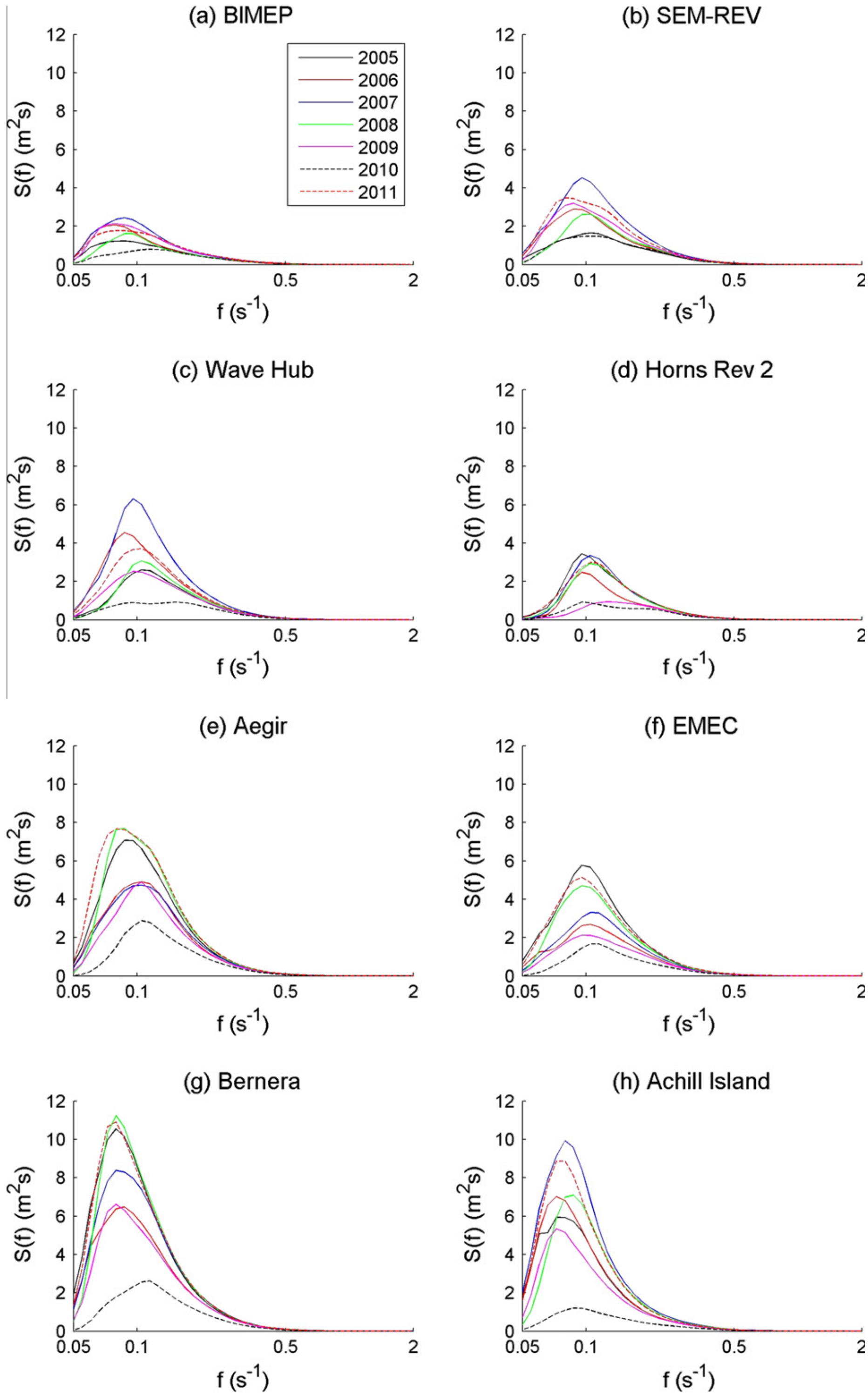

Fig. 12. One-dimensional winter (December–January–February) mean wave spectra for eight locations distributed around the NW European shelf seas.

sea limits, whereas our study covers the entire NW European shelf seas. However, if we interpolate our high-resolution gridded model outputs to the data points covered by the Atlas, we can compare the annual mean wave power estimated by the two studies. Since we have simulated different dates (January 2005–December 2011) than those dates analysed to produce the Atlas (June 2000–May 2007), it is appropriate to normalise the results of each study by the wave power averaged over all of the data points covered by the Atlas. The normalised comparison falls closely to the line of equality (Fig. 15), and so the two studies are comparable. However, when comparing non-normalised outputs between the two studies, we found that the mean annual wave power from our study is around 10% lower than that estimated by the Atlas. This can partly be explained by variability of the wind (and hence wave) climates over the different time periods used for the two studies. For example, the mean DJF NAO used for the Atlas was +0.21, compared to −0.32 used for this study. Based on the equation describing the line of best fit on Fig. 14, this could account for around 10%

Table 4
Inter-annual variability of peak wave period *Tp* (s) at each of eight wave energy project locations averaged over winter months (December–January–February), and over the entire year. Values in each cell of the table are given as $w(a)$: w = winter mean, a = annual mean.

Project	Peak wave period *Tp* (s)						
	2005	2006	2007	2008	2009	2010	2011
BIMEP	11.5(11.5)	12.6(11.5)	11.5(11.5)	10.5(10.5)	12.6(11.5)	8.7(10.5)	12.6(11.5)
SEM-REV	9.6(8.7)	11.5(9.6)	10.5(10.5)	9.6(9.6)	11.5(10.5)	9.6(10.5)	12.6(8.7)
Wave Hub	9.6(8.7)	11.5(10.5)	10.5(10.5)	9.6(8.7)	10.5(9.6)	6.6(9.6)	9.6(8.7)
Horns Rev 2	10.5(9.6)	10.5(9.6)	9.6(9.6)	9.6(8.7)	8.0(8.7)	10.5(8.7)	9.6(8.7)
Aegir	11.5(10.5)	9.6(9.6)	9.6(9.6)	11.5(10.5)	9.6(9.6)	9.6(9.6)	12.6(10.5)
EMEC	10.5(10.5)	9.6(9.6)	9.6(9.6)	10.5(9.6)	10.5(9.6)	8.7(8.7)	10.5(9.6)
Bernera	12.6(11.5)	11.5(11.5)	12.6(11.5)	12.6(11.5)	12.6(11.5)	8.7(9.6)	12.6(11.5)
Achill Island	13.8(11.5)	13.8(12.6)	12.6(12.6)	11.5(11.5)	13.8(12.6)	11.5(11.5)	12.6(11.5)

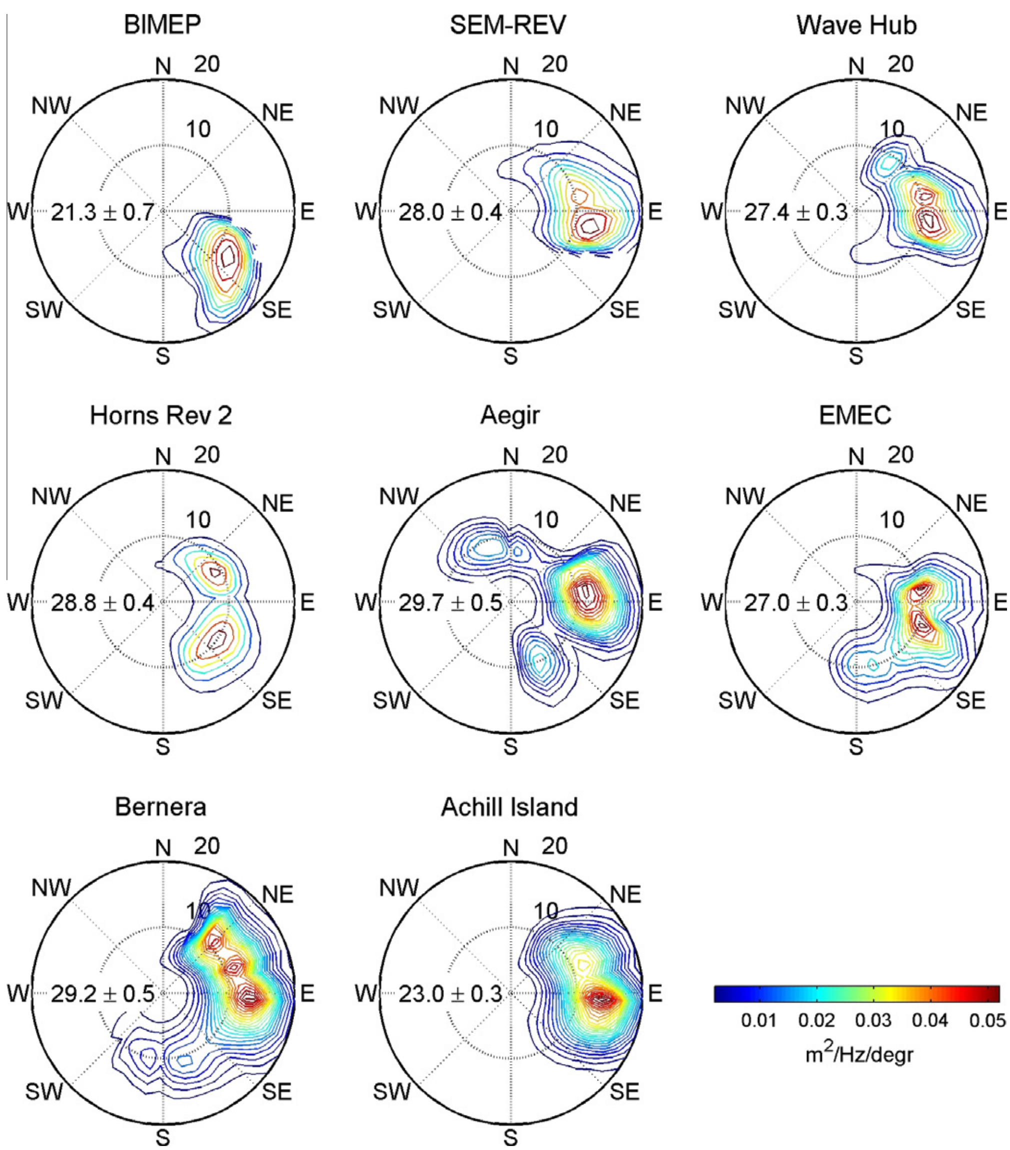

Fig. 13. Annual mean two-dimensional wave spectra (calculated for period 2005–2011) for eight locations distributed around the NW European shelf seas. The radial coordinate is wave period(s), and contours are variance densities in $m^2/Hz/°$. The numbers on each plot are the mean directional spreading (in degrees), including the 90% confidence intervals.

discrepancy during the winter months. Further, there were considerable discrepancies between model configurations used in each of the two studies. There are differences in spatial resolution ($1/24° \times 1/24°$ in our study, compared to $1/6° \times 1/9°$ for the Atlas), frequency resolution (40 frequency bins in our study, compared to 13 frequency bins for the Atlas), and directional resolution (45 discrete direction bins for our study, compared to 16 direction bins for the Atlas). However, perhaps more fundamental is the choice of wave model. The Atlas is based on analysis of outputs from a second-generation wave model, whereas our study uses a

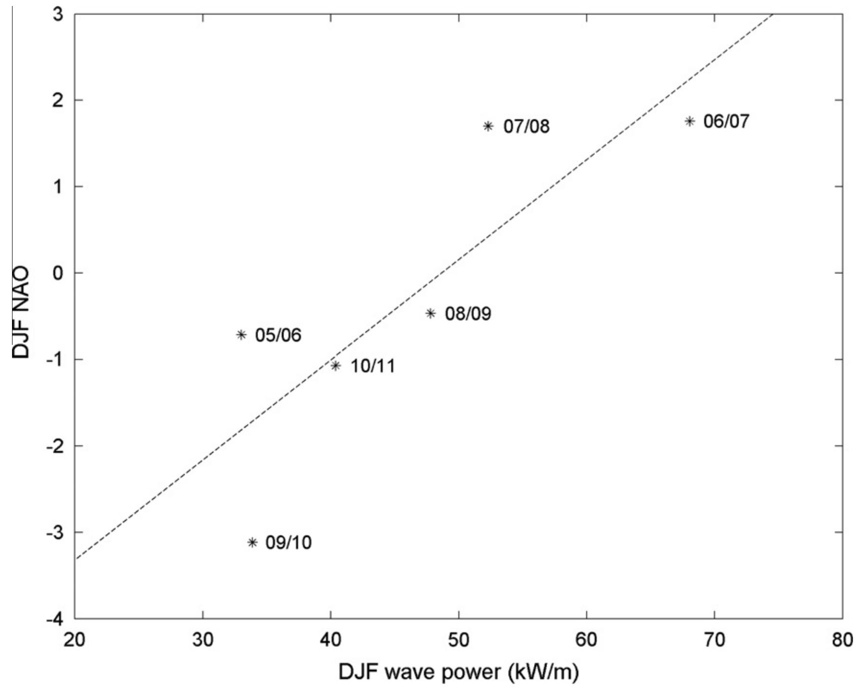

Fig. 14. Mean winter (December–January–February) wave power averaged over the NW European shelf seas plotted against the DJF NAO. The dashed line is the least squares line of best fit (r^2 = 0.69).

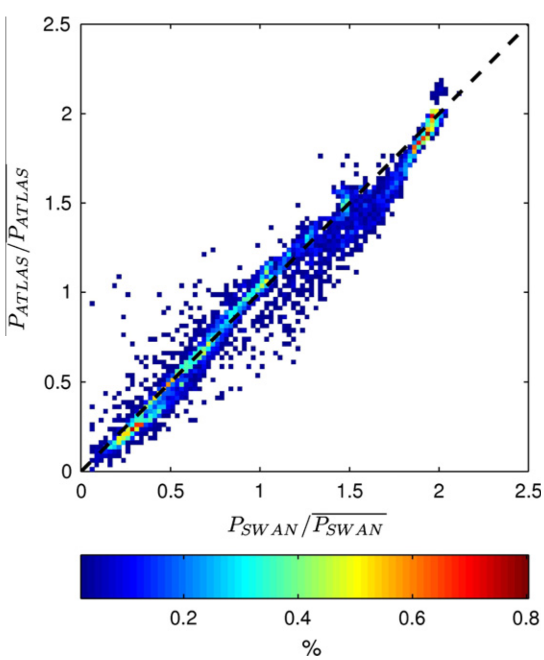

Fig. 15. Comparison of annual mean wave power estimated by this study and the UK Atlas of Marine Renewable Energy Resources plotted as percentage probability. Since a different time period was used for each resource assessment, wave power at each data point has been normalised by the spatial mean. The equality line at 45° is shown as a dashed line.

third-generation wave model. One of the key differences between a 2nd and 3rd generation wave model is more accurate representation of non-linear wave-wave interactions. In particular, 3rd generation wave models explicitly calculate quadruplet wave-wave interactions, rather than parameterising such non-linear process [32]. Quadruplet wave-wave interactions redistribute a significant fraction of the wind input from the mid-range frequencies to lower frequencies, and a smaller fraction to higher frequencies [33], the energy of which is then dissipated by other physical process which have improved representation in 3rd generation wave models, e.g. white-capping. Our results therefore indicate that the 2nd generation wave model which was used to compile the Atlas of UK Marine Renewable Energy Resources may have over-estimated wave power. It is interesting to note that in the same year that the Atlas was published (2008), the UK Met Office implemented a third-generation wave model (WAVEWATCH III) as a replacement for the Met Office second-generation operational wave model.

6. Conclusions

Our high resolution third-generation SWAN wave model simulations, applied to 7 years of wind forcing, provide a realistic assessment of the NW European wave resource. We have examined inter-annual and inter-seasonal variability, and compared the wave power resource for contrasting regions of the NW European shelf seas. This thorough assessment, including the analysis of wave spectra for sites where wave energy projects are under development, quantifies variability of the NW European wave resource, and so provides potential developers with statistics relevant to matching each site to the most appropriate wave energy converter (WEC) technology.

Our analysis demonstrates that there is considerably more uncertainty in the wave resource from October to March, in contrast to the lower April–September uncertainty. The strong correlation between wave power over the winter months and large-scale modes of natural climate variability demonstrates that the North Atlantic Oscillation (NAO) is a good indicator of the NW European shelf sea winter wave power resource, provided that trends in the NAO can be identified with any certainty over the coming decades.

Model studies like this can generally be improved by increasing model resolution. However, our spatial resolution of $1/24° \times 1/24°$ over the entire NW European shelf seas already represents a significant advancement on previous resource assessments which include parts of the study region, since these models had spatial resolutions of $1/6^\circ \times 1/9^\circ$ [9], and $1/5^\circ \times 1/5^\circ$ [6]. Finally, our use of the third-generation wave model SWAN, compared to a previous resource assessment of a large part of the study region which was based on analysing outputs from a second-generation wave model, has improved the representation of the physical processes, particularly non-linear wave-wave interactions. We believe that considering the advances in computing power, availability of wind data, and the urgency with which we must move towards generating electricity from low carbon technologies, it is timely to produce an updated high-resolution atlas of the NW European shelf sea wave energy resource, and this research represents a first step towards creating such a resource.

Acknowledgements

Thanks to the British Oceanographic Data Centre (BODC) for supplying the GEBCO bathymetry data, to Met Éireann for supplying gridded wind data, and to the European Centre for Medium-Range Weather Forecasting (ECMWF) for supplying a longer time-series of significant wave height for the North Atlantic. Wave buoy data used for model validation was provided by the Irish Marine Institute and BODC, and data on the North Atlantic Oscillation were provided by the Climatic Research Unit at the University of East Anglia. Data from the Atlas of UK Marine Renewable Energy Resources was provided by ABPmer. The extensive model simulations were made possible by access to High Performance Computing (HPC) Wales, a collaboration between Welsh universities, the Welsh Government and Fujitsu. This work was undertaken as part of the Low Carbon Research Institute Marine Consortium. The Authors wish to acknowledge the financial support of the Welsh Government, the Higher Education Funding Council for Wales, the Welsh European Funding Office, and the European Regional Development Fund Convergence Programme.

References

[1] Bahaj AS. Generating electricity from the oceans. Renew Sust Energy Rev 2011;15:3399–416.
[2] Gunn K, Stock-Williams C. Quantifying the global wave power resource. Renew Energy 2012;44:296–304.
[3] Clément A, McCullen P, Falcão A, Fiorentino A, Gardner F, Hammarlund K, et al. Wave energy in Europe: current status and perspectives. Renew Sust Energy Rev 2002;6:405–31.
[4] Bryden IG, Melville GT. Choosing and evaluating sites for tidal current development. Proc Inst Mech Eng Part A: J Power Energy 2004;218:567–77.
[5] Carretero JC, Gomez M, Lozano I, de Elvira AR, Serrano O, Iden K, et al. Changing waves and storms in the northeast Atlantic? Bull Amer Meteorol Soc 1998;79:741–60.
[6] Reeve DE, Chen Y, Pan S, Magar V, Simmonds DJ, et al. An investigation of the impacts of climate change on wave energy generation: the Wave Hub, Cornwall, UK. Renew Energy 2011;36:2404–13.
[7] Charles E, Idier D, Delecluse P, Déqué M, Le Cozannet G. Climate change impact on waves in the Bay of Biscay, France. Ocean Dynam 2012;62:831–48.
[8] Jeffrey H, Sedgwick J. ORECCA European offshore renewable energy roadmap. Published by the ORECCA Coordinated Action Project, University of Edinburgh; 2011.
[9] ABPmer, The Met Office, Proudman Oceanographic Laboratory. Atlas of UK marine renewable energy resources. Tech. rep., Department for Business Enterprise & Regulatory Reform; 2008.
[10] Akpinar A, Komurcu MI. Assessment of wave energy resource of the Black sea based on 15-year numerical hindcast data. Appl Energy 2013;101:502–12.
[11] Bernhoff H, Sjostedt E, Leijon M. Wave energy resources in sheltered sea areas: a case study of the Baltic Sea. Renew Energy 2006;31:2164–70.
[12] Iglesias G, Carballo R. Wave resource in El Hierro – an island towards energy self-sufficiency. Renew Energy 2011;36:689–98.
[13] Hughes MG, Heap AD. National-scale wave energy resource assessment for Australia. Renew Energy 2010;35:1783–91.
[14] Zheng CW, Zhuang H, Li X, Li XQ. Wind energy and wave energy resources assessment in the East China Sea and South China Sea. Sci China – Technol Sci 2012;55:163–73.
[15] EPRI. Mapping and assessment of the United States ocean wave energy resource. Technical report 1024637, Electrical Power Research Institute, Palo Alto, CA; 2011.
[16] Cooper WS, Hinton CL, Ashton N, Saulter A, Morgan C, Proctor R, et al. An introduction to the UK marine renewable atlas. Proc Inst Civil Eng – Marit Eng 2006;159:1–7.
[17] Cornett AM. A global wave energy resource assessment. In: Proceedings of the 18th ISOPE conference, Vancouver, BC, Canada; 2008. p. 1–9.
[18] Liberti L, Carillo A, Sannino G. Wave energy resource assessment in the Mediterranean, the Italian perspective. Renew Energy 2013;50:938–49.
[19] Izadparast AH, Niedzwecki JM. Estimating the potential of ocean wave power resources. Ocean Eng 2011;38:177–85.
[20] Iglesias G, Carballo R. Wave resource characterization and WEC selection a comprehensive methodology applied to NW Spain. In: Proceedings of the 9th European wave and tidal energy conference, Southampton, UK; 2011. p. 1–8.
[21] Kofoed JP, Frigaard P, Friis-Madsen E, Chr. Srensen H. Prototype testing of the wave energy converter wave dragon. Renew Energy 2006;31:181–9.
[22] Neill SP, Scourse JD, Bigg GR, Uehara K. Changes in wave climate over the northwest European shelf seas during the last 12,000 years. J Geophys Res – Oceans 2009;114:C06015.
[23] Mouslim H, Babarit A, Clément A, Borgarino B. Development of the French wave energy test site SEM-REV. In: Proceedings of the 8th European wave and tidal energy conference, Uppsala, Sweden; 2009. p. 31–5.
[24] Beels C, Henriques JCC, de Rouck J, Pontes MT, de Backer G, Verhaeghe, H. Wave energy resource in the North Sea. In: Proceedings of the 7th European wave and tidal energy conference, Porto, Portugal; 2007. p. 1–10.
[25] http://www.aquamarinepower.com/projects/west-coast-ireland; 2012 [accessed 06.09.12].
[26] Palutikof J, Holt T, Skellern A. Wind: resources and hazard. In: Hulme M, Barrow E, editors. Climates of the British Isles. London: Routledge; 1997. p. 220–42.
[27] Barrow E, Hulme M. Describing the surface climate of the British Isles. In: Hulme M, Barrow E, editors. Climates of the British Isles. London: Routledge; 1997. p. 33–62.
[28] Draper L. Wave climatology of the UK continental shelf. In: Banner FT, Collins MB, Massie KS, editors. The north-west European shelf seas: the sea bed and the sea in motion. II. Physical and chemical oceanography, and physical resources. Elsevier; 1980. p. 353–68.
[29] Hurrell JW. Decadal trends in the North-Atlantic Oscillation – regional temperatures and precipitation. Science 1995;269:676–9.
[30] Mackay EBL, Bahaj AS, Challenor PG. Uncertainty in wave energy resource assessment. Part 2: Variability and predictability. Renew Energy 2010;35:1809–19.
[31] Neill SP, Scourse J, Uehara K. Evolution of bed shear stress distribution over the northwest European shelf seas during the last 12,000 years. Ocean Dynam 2010;60:1139–56.
[32] Booij N, Ris RC, Holthuijsen LH. A third-generation wave model for coastal regions – 1. Model description and validation. J Geophys Res 1999;104:7649–66.
[33] Holthuijsen LH. Waves in oceanic and coastal waters. Cambridge University Press; 2009.
[34] Pinson P, Reikard G, Bidlot JR. Probabilistic forecasting of the wave energy flux. Appl Energy 2012;93:364–70.
[35] Saulnier JB, Maisondieu C, Ashton I, Smith GH. Refined sea state analysis from an array of four identical directional buoys deployed off the Northern Cornish coast (UK). Appl Ocean Res 2012;37:1–21.
[36] Meehl GA, Tebaldi C. More intense, more frequent, and longer lasting heat waves in the 21st century. Science 2004;305:994–7.
[37] Trigo RM, Osborn TJ, Corte-Real JM. The North Atlantic Oscillation influence on Europe: climate impacts and associated physical mechanisms. Clim Res 2002;20:9–17.
[38] Bojariu R, Gimeno L. Predictability and numerical modelling of the North Atlantic Oscillation. Earth-Sci Rev 2003;63:145–68.